Primordial black hole formation in the early universe: critical behaviour and self-similarity

Ilia Musco[1] **and John C. Miller**[2,3]

[1]Centre of Mathematics for Applications, Department of Mathematics, University of Oslo, PO Box 1053 Blindern, NO-0316 Oslo, Norway

[2] Department of Physics (Astrophysics), University of Oxford, Keble Road, Oxford OX1 3RH, UK

[3] SISSA, International School for Advanced Studies and INFN, Via Bonomea 265, I-34136 Trieste, Italy

Abstract. Following on after three previous papers discussing the formation of primordial black holes during the radiation-dominated era of the early universe, we present here a further investigation of the critical nature of the collapse. In particular, we focus on the long-lived intermediate state, which appears in collapses of perturbations close to the critical limit, and examine the extent to which this follows a similarity solution, as seen for critical collapse under more idealized circumstances (rather than within the context of an expanding universe, as studied here). We find that a similarity solution is indeed realised, to good approximation, for a region contained within the past light-cone of the forming black hole (and eventual singularity). The self-similarity is not exact, however, and this is explained by the presence within the light-cone of some outer matter still coupled to the expanding universe, which does not participate in the self-similarity. Our main interest, from a cosmological point of view, is in a radiative fluid with equation of state parameter $w = 1/3$ (when the pressure p and energy density e are taken to be related by $p = we$). Other values of w, in the range $0 - 1$, have also been considered in the literature on critical collapse and we have looked at some of these too, within the context of our calculations, with the aim of gaining further insight into our main case of interest. As expected, we find that the features of scaling-law behaviour, intermediate state and similarity solution are preserved in all of the cases studied but with some interesting variations in the details. As in our previous work, we have started our simulations with initial supra-horizon scale perturbations of a type which could have come from inflation.

PACS numbers: 04.70.-s, 98.80.Cq

Submitted to: *Class. Quantum Grav.*

1. Introduction

A population of primordial black holes (PBHs) might have been formed in the early universe due to gravitational collapse of large-enough cosmological perturbations. Following the initial papers suggesting this (Zel'dovich & Novikov (1969) [1]; Hawking (1971) [2]; Carr [3, 4]), various authors then investigated the process numerically (Nadezhin, Novikov & Polnarev (1978) [5]; Bicknell & Henriksen (1979) [6]; Novikov & Polnarev (1980) [7] Niemeyer and Jedamzik (1999) [8]; Shibata and Sasaki (1999) [9]; Hawke & Stewart (2002) [10]; Musco, Miller & Rezzolla (2005) [11]). PBHs would have been formed if some cosmological perturbations had reached an amplitude δ, at the time of cosmological horizon crossing, greater than a certain threshold value δ_c (the δ is often defined as the relative mass excess inside the overdense region, measured at the time of horizon crossing). The simulations clarified many different aspects of the nature of the collapse, with particular reference to the radiative era of the universe (with the equation of state being taken as $p = \frac{1}{3}e$, where p is the pressure and e is the energy density). This context represents the most commonly studied scenario for PBH formation.

Niemeyer & Jedamzik (1999) [8, 12] showed that the masses of PBHs produced in the radiative era by perturbations of a given profile type, follow the typical scaling-law behaviour of critical collapse, first discovered for idealized conditions by Choptuik (1993) [14], i.e. the masses of the black holes produced follow a power law $M_{BH} \propto (\delta - \delta_c)^\gamma$ if δ is close enough to δ_c. Neilsen & Choptuik (2000) [15] later showed that one could get a critical collapse, using a succession of "imploding shells" of matter as the initial conditions, for $p = we$ equations of state with any w in the range $0 - 1$. For these configurations, they found that the value of the critical exponent γ was dependent only on the value of w and not on the particular form of the perturbation profile.

In 2002, Hawke & Stewart [10] came back to the problem of critical collapse in the context of PBH formation in the early universe with a radiative fluid, and investigated the nature of the collapse going down to smaller values of $(\delta - \delta_c)$ than Niemeyer & Jedamzik had been able to do with their code. For the larger values of $(\delta - \delta_c)$, comparable to those of [8], Hawke & Stewart again found a scaling law with a similar value of γ, but for smaller $(\delta - \delta_c)$ they saw formation of strong shocks and the curve flattened off at a minimum mass of around 10^{-3} of their horizon mass. They also found that the value of δ_c depended strongly on the shape of the perturbation, in contrast to [8].

In Musco et al (2005) [11], we considered PBH formation with initial conditions given by linear perturbations of the energy density and velocity fields approximating the growing components of cosmological perturbations, and imposed with a length-scale much larger than the cosmological horizon. The domination of the growing component becomes even greater by the time of horizon crossing, as any residual decaying component dies away. We again saw a scaling law with similar γ for the range of values of $(\delta - \delta_c)$ used by [8] but found very different values of δ_c from [8] for similar perturbation shapes (we were concentrating on those types of perturbation).

This difference was attributed to the fact that in [8], the perturbations were made just in the energy density and were imposed directly at the horizon scale, so that their value of δ_c was calculated with inclusion of a substantial decaying component which did not then contribute to the black hole formation. If one focuses on the effect of perturbations originating from inflation, then it is clearly only growing components which are relevant at much later times.

In Polnarev & Musco (2007) [16], this kind of cosmologically-relevant initial perturbation was imposed in a more precise way, using an asymptotic quasi-homogeneous solution [17]. Starting from a curvature perturbation, which is a time-independent quantity when the perturbation length-scale is much larger than the cosmological horizon [18], perturbations in all of the other quantities can then be specified in a consistent way, giving a solution with only a growing component. The metric perturbation can be large even when the perturbations in energy density and velocity are small, and only when there is a large-amplitude metric perturbation, corresponding to a non-linear initial perturbation of the curvature, can one get $\delta > \delta_c$ at horizon crossing.

In Musco et al (2009) [19], we returned to the issue raised by Hawke & Stewart [10] concerning whether the scaling law would continue down to very small values of $(\delta - \delta_c)$. In order to address this, we needed to modify our code with the inclusion of adaptive mesh refinement (AMR) so as to be able to handle the extreme conditions which arise near to the critical limit. In view of our earlier work, we were particularly wanting to investigate the effect of using initial perturbations with just a growing component imposed outside the horizon scale, rather than the non-linear sub-horizon scale initial perturbations used in [10]. We again used the quasi-homogeneous solution to provide our initial conditions. Doing this, we did not observe the shock formation seen in [10] (which we attributed to the presence of a non-linear decaying component in their calculations) but instead got a regular scaling law behaviour all the way down to the vicinity of the resolution limit of our scheme (going beyond the most extreme values shown in [10]). A striking feature of our calculations was the appearance of an "intermediate state" during collapse for cases near to the critical limit: the collapse proceeded to a compactness $2M/R \sim 0.5$ (where R and M are the current radius and mass of the condensation) which then remained roughly constant for a large number of dynamical timescales, with the condensation progressively shedding matter via a relativistic wind and shrinking, until eventually it either reached a mass at which the final collapse to a black hole could take place or started to disperse.

The existence of a similarity solution, for collapses near to the critical limit, is a key feature of the theory of critical collapse [20, 21], and in [19] we saw some evidence of self-similarity also in the context of PBH formation within an expanding universe. This is associated with the long-lived intermediate state. In the present paper, we return to investigate this further, focusing on the intermediate state and examining the extent to which it does, in fact, follow a similarity solution. We also investigate other values of w. While our main interest from a cosmological point of view is in $w = 1/3$, it is useful to

look at other values as well, using the same approach, so as to get further insight into the main case of interest. Also, other values of w might be relevant for PBH formation at certain particular times in the early universe.

The results presented in this paper have been obtained using the same numerical code as in [19], with some fine tuning of the AMR and modifications for calculating the past light cone of the forming black hole. After this Introduction, Section 2 reviews our mathematical formulation of the problem, Section 3 contains a brief summary of the numerical methods used and also a description of our newly-introduced calculation of the past light cone; Section 4 presents results from our investigations of the intermediate state and the similarity solution, and of the consequences of using different values for w; Section 5 gives conclusions. In an Appendix, we discuss the concepts of cosmological and black-hole horizons within the present treatment. Throughout, we use units for which $c = G = 1$, except where otherwise stated.

2. Mathematical formulation of the problem

2.1. Cosmic-time slicing

For the calculations described here, we have followed the same basic methodology as described in our previous papers [11, 16, 19] (which we will refer to as Papers 1, 2 and 3 respectively). We therefore give just a brief summary of it here; more details are contained in the previous papers.

We use two different formulations of the general relativistic hydrodynamic equations: one for setting the initial conditions and the other for studying the black hole formation. Throughout, we are assuming spherical symmetry and that the medium can be treated as a perfect fluid; we use a Lagrangian formulation of the equations with a radial coordinate r which is co-moving with the matter.

For setting the initial conditions, it is convenient to use a diagonal form of the metric, with the time coordinate t reducing to the standard Friedmann-Robertson-Walker (FRW) time in the case of a homogeneous medium with no perturbations. (This sort of time coordinate is therefore often referred to as "cosmic time"). We write this metric in the form given by Misner & Sharp (MS) [22], whose approach we follow here in writing the GR hydrodynamic equations:

$$ds^2 = -a^2\,dt^2 + b^2\,dr^2 + R^2\left(d\theta^2 + \sin^2\theta d\varphi^2\right)\,, \tag{1}$$

with the coefficients a, b and R being functions of r and t and with R playing the role of an Eulerian radial coordinate. Using the definitions

$$D_t \equiv \frac{1}{a}\left(\frac{\partial}{\partial t}\right)\,, \tag{2}$$

$$D_r \equiv \frac{1}{b}\left(\frac{\partial}{\partial r}\right)\,, \tag{3}$$

one defines the quantities

$$U \equiv D_t R\,, \tag{4}$$

and

$$\Gamma \equiv D_r R\,, \tag{5}$$

where U is the radial component of four-velocity in the "Eulerian" frame and Γ is a generalized Lorentz factor. The metric coefficient b can then be written as

$$b \equiv \frac{1}{\Gamma}\frac{\partial R}{\partial r}\,, \tag{6}$$

With these specifications, the GR hydrodynamic equations can be written in the following form (with the notation that e is the energy density, p is the pressure, ρ is the compression factor and M is the mass contained inside radius R):

$$D_t U = -\left[\frac{\Gamma}{(e+p)} D_r p + \frac{M}{R^2} + 4\pi R p\right]\,, \tag{7}$$

$$D_t \rho = -\frac{\rho}{\Gamma R^2} D_r (R^2 U),\,, \tag{8}$$

$$D_t e = \frac{e+p}{\rho} D_t \rho\,, \tag{9}$$

$$D_t M = -4\pi R^2 p U\,, \tag{10}$$

$$D_r a = -\frac{a}{e+p} D_r p\,, \tag{11}$$

$$D_r M = 4\pi R^2 \Gamma e\,, \tag{12}$$

plus a constraint equation

$$\Gamma^2 = 1 + U^2 - \frac{2M}{R}\,. \tag{13}$$

An equation of state is also needed, and we are here considering ones of the form

$$p = we\,, \tag{14}$$

where w is a constant parameter which can take various values. When a cosmological constant is added, the total energy density $\tilde{e}$ and the total pressure $\tilde{p}$ are given by

$$\tilde{e} = e + \frac{\Lambda}{8\pi} \qquad\qquad \tilde{p} = p - \frac{\Lambda}{8\pi}\,, \tag{15}$$

where $\Lambda/8\pi$ is the additional vacuum component of the energy density and $-\Lambda/8\pi$ is the vacuum component of the pressure; these vacuum contributions satisfy (14) with $w = -1$. The cosmological constant produces a gravitational effect that changes the background, but does not affect the fluid in other ways.

2.2. Initial conditions

The initial conditions are set by introducing a perturbation of the otherwise uniform medium representing the cosmological background solution, with the length-scale of the perturbation R_0 being much larger than the cosmological horizon $R_H \equiv H^{-1}$. Under these circumstances, the perturbations in e and U can be extremely small while still giving a large-amplitude perturbation of the metric (as is necessary if a black hole is eventually to be formed) and the above system of equations can then be solved analytically to first order in the small parameter $\epsilon \equiv (R_H/R_0)^2 \ll 1$. A full discussion of this has been given in Paper 2. The result obtained, referred to as the "quasi-homogeneous solution", gives formulae for the perturbations of all of the metric and hydrodynamical quantities in terms only of a curvature perturbation profile $K(r)$ that is conveniently time-independent when $\epsilon \ll 1$ [18].

To characterize the amplitude of the perturbation, we use the integrated quantity

$$\delta(t) = \left(\frac{4}{3}\pi r_0^3\right)^{-1} \int_0^{r_0} 4\pi r^2 \left(\frac{e(r,t) - e_b(t)}{e_b(t)}\right) dr\,, \tag{16}$$

which measures the relative mass excess within the overdense region, as frequently done in the literature; e_b is the background value of the energy density and r_0 is the co-moving length-scale of the overdense region of the perturbation, determined by the particular expression used for K(r). In Paper 2 (to which we refer for details) it was shown that

$$\frac{e(r,t) - e_b(t)}{e_b(t)} \;=\; \epsilon(t)\frac{3(1+w)}{5+3w}\frac{r_0^2}{3r^2}\frac{\partial\left[r^3 K(r)\right]}{\partial r}\,, \tag{17}$$

and here, as in Paper 3, we make the simplest choice of using a Gaussian for the initial curvature profile $K(r)$,

$$K(r) = \exp\left(-\frac{r^2}{2\Delta^2}\right)\,, \tag{18}$$

which implies $r_0^2 = 3\Delta^2$ and leads to the corresponding Mexican Hat profile for the energy density at the initial time:

$$K(r) = \exp\left(-\frac{3}{2}\left(\frac{r}{r_0}\right)^2\right) \tag{19}$$

$$\frac{e(r,t) - e_b(t)}{e_b(t)} \;=\; \epsilon(t)\frac{3(1+w)}{5+3w}\Delta^2\left[1 \;-\; \left(\frac{r}{r_0}\right)^2\right]\exp\left(-\frac{3}{2}\left(\frac{r}{r_0}\right)^2\right), \tag{20}$$

where Δ is the free parameter used at the initial time to vary the perturbation amplitude. Inserting (20) into (16) one gets

$$\delta(t) = \epsilon(t)\frac{9(1+w)}{5+3w}\Delta^2\exp\left(-\frac{3}{2}\right), \tag{21}$$

within the linear regime where $\epsilon \ll 1$, with the time evolution of the perturbation being given only by $\epsilon(t)$, which measures how the cosmological horizon R_H grows with respect to the length-scale of the perturbation R_0. Inserting the expression for $\epsilon(t)$ gives

$$\delta(t) = \delta(t_i)\left(\frac{t}{t_i}\right)^{\frac{2(1+3w)}{3(1+w)}}\,, \tag{22}$$

which leads to the familiar relationships $\delta(t) \propto t$ when $w = 1/3$ and $\delta(t) \propto t^{2/3}$ when $w = 0$. Full details about setting initial conditions using the quasi-homogeneous solution are given in Paper 2.

For our subsequent discussion of the scaling laws, we need a value for δ measured at a standard time and it is convenient to take this as being the time at which $\epsilon(t) = 1$. For small perturbations, this coincides with the horizon-crossing time, and it does not differ by very much from that even for the larger perturbations of interest for PBH formation, at least for the type of perturbation profile being used here. Since evaluating (21) analytically is much more precise than making a numerical integral on the grid at horizon-crossing time, we use that value for the discussion of the scaling laws, as we did in Papers 2 and 3.

Profiles similar to a Mexican Hat for the energy density perturbation represent a plausible and simple choice, and previous studies [13, 11, 16] have shown that other centred peak perturbation profiles, such as polynomial ones, behave in a very similar way, giving almost the same values for δ_c. Off-centred profiles could, in principle, give rise to more substantial changes but are rather unlikely to arise naturally. Therefore, in the absence of any strong motivation for considering those kinds of profile, we restrict our choice of initial conditions only to Mexican Hat profiles given by (20).

2.3. Observer-time slicing

The MS approach using cosmic time slicing is convenient for setting initial conditions but has the well-known drawback for calculations of black hole formation that singularities are formed rather quickly when using it and further, potentially observable, evolution cannot then be followed unless an excision procedure is used. Various slicing conditions can be used to avoid this difficulty but for calculations in spherical symmetry it is particularly convenient to use null slicing. In our work we have used the "observer time" null-slicing formulation of Hernandez & Misner [24] where the time coordinate is taken as the time at which an outgoing radial light ray emanating from an event reaches a distant observer. (In the original formulation, this observer was placed at future null infinity but for calculations in an expanding cosmological background we use an FRW fundamental observer sufficiently far from the perturbed region so as to be unaffected by the perturbation.) We use the MS approach for setting up initial data and for evolving it so as to produce data on a null slice. This is then used as input for our observer-time code with which we follow the black hole formation.

For the observer-time calculation, the metric (1) is re-written as

$$ds^2 = -f^2\,du^2 - 2fb\,dr\,du + R^2\left(d\theta^2 + \sin^2\theta d\varphi^2\right)\,, \tag{23}$$

where u is the observer time and f is the new lapse function. The operators equivalent to (2) and (3) are now

$$D_t \equiv \frac{1}{f}\left(\frac{\partial}{\partial u}\right)\,, \tag{24}$$

$$D_k \equiv \frac{1}{b}\left(\frac{\partial}{\partial r}\right) , \tag{25}$$

where D_k is the radial derivative in the null slice and the corresponding derivative in the Misner-Sharp space-like slice is given by

$$D_r = D_k - D_t \, . \tag{26}$$

The hydrodynamic equations can then be formulated in a way analogous to what was done in cosmic time. The observer-time equations used in the code, replacing the cosmic-time ones (7) – (12), are:

$$D_t U = -\frac{1}{1-c_s^2}\left[\frac{\Gamma}{(e+p)}D_k p + \frac{M}{R^2} + 4\pi R p + c_s^2\left(D_k U + \frac{2U\Gamma}{R}\right)\right] , \tag{27}$$

$$D_t \rho = \frac{\rho}{\Gamma}\left[D_t U - D_k U - \frac{2U\Gamma}{R}\right] , \tag{28}$$

$$D_t e = \left(\frac{e+p}{\rho}\right) D_t \rho \, , \tag{29}$$

$$D_k\left[\frac{(\Gamma+U)}{f}\right] = -4\pi R(e+p) f \, . \tag{30}$$

$$D_k M = 4\pi R^2 [e\Gamma - pU], \tag{31}$$

where $c_s = \sqrt{(\partial p/\partial e)} = \sqrt{w}$ is the sound speed. The quantity Γ is given by (13), as before, and we also have

$$\Gamma = D_k R - U \, , \tag{32}$$

which replaces (5) in this slicing.

3. The method of calculation

The present calculations have been made with the same code as used in Paper 3. Since this has been fully described previously, we will just give a brief outline of it here. It is an explicit Lagrangian hydrodynamics code based on that of Miller & Motta (1989) [25] but with the grid organized in a way similar to that of Miller & Rezzolla (1995) [26] which was designed for calculations in an expanding cosmological background. The code has a long history and has been carefully tested in its various forms. The basic grid uses logarithmic spacing in a mass-type comoving coordinate, allowing it to reach out to very large radii while giving finer resolution at small radii. Our initial data is derived from the quasi-homogeneous solution and is specified on a space-like slice (at constant cosmic time) with $\epsilon = 10^{-2}$, giving $R_0 = 10\, R_H$. The outer edge of the grid has usually been placed at $90\, R_H$, which is far enough away so that there is no causal contact between it and the perturbed region during the time of the calculations. The

initial data is then evolved using the MS equations (7-13), so as to generate a second set of initial data on a null slice (at constant observer time) and the null-slice initial data is then evolved using the observer-time equations [11].

For the calculations presented in Paper 3, we introduced an adaptive mesh refinement scheme (AMR), on top of the existing logarithmic grid, giving us sufficient resolution so as to be able to follow black hole formation down to extremely small values of $(\delta - \delta_c)$. Having the AMR is particularly important for allowing us to follow the deep voids which form outside the central collapsing region in cases very close to the critical limit. The same scheme has been used with just minor modifications for the calculations presented here. Our aim in writing the AMR was to avoid the use of artificial viscosity, but it has now emerged that some residual artificial viscosity was still present and is necessary for correct functioning of the code in its present form. The presence of this is not thought to affect the results presented in any important way, however. We have successfully used the scheme with more than thirty levels of refinement and all relevant features of the solutions have been fully resolved.

For the discussion of the similarity solutions in the next section, we are needing to know the location of the past light cone of the forming black hole (and of the eventual singularity). This involves tracing the paths of ingoing radial light rays. Considering the observer-time metric (23): along radial null rays, we have $ds = d\theta = d\varphi = 0$, so that

$$f^2\, du^2 + 2fb\, dr\, du = 0\,, \tag{33}$$

giving

$$f du(f du + 2b dr) = 0\,. \tag{34}$$

This has two solutions: $du = 0$, referring to an *outgoing* radial null ray (the basic definition for the observer-time as the time at which events are seen by a distant observer), and $dr = -(f/2b)du$ for an *ingoing* null ray. The general expression for changes in R along a radial worldline is

$$dR = \frac{\partial R}{\partial u} du + \frac{\partial R}{\partial r} dr\,. \tag{35}$$

Using (4), (5) and (24) - (26) one has

$$\frac{\partial R}{\partial u} = fU \qquad \text{and} \qquad \frac{\partial R}{\partial r} = b(\Gamma + U)\,, \tag{36}$$

and inserting these into (35) gives

$$dR = fU\, du + b(\Gamma + U)\, dr\,, \tag{37}$$

which, with the relation $dr = -(f/2b)du$, leads to

$$\frac{dR}{du} = \frac{f}{2}(U - \Gamma)\,, \tag{38}$$

along an ingoing radial null ray.

The use of observer time gives a particularly clear treatment of light cones. We are interested in the past light cone of the asymptotically-forming black hole (which would

also then be the lightcone of the subsequent singularity). Our code does not allow us to make an evolution backwards in time, however, and so we need to find the location of this light cone at our initial time by means of an iterative process, looking for the ingoing light-ray which settles into the surface of the black hole at formation. We used a secant iteration for doing this.

4. Results: intermediate state, similarity solutions and variation of w

In this section, we present results from our further investigation of the intermediate state including, in particular, examining the extent to which it follows a similarity solution. We also investigate the effects of using values of w different from 1/3. As mentioned previously, while our main interest from a cosmological point of view is in $w = 1/3$, it is useful to look at other values as well, using the same approach, so as to gain further insight into the main case of interest. Some of these other values might also be directly relevant at some particular stages in the early universe.

After a growing perturbation enters within the cosmological horizon, it will start to contract and then collapse if its amplitude δ is large enough. If δ is larger than the critical value δ_c, it will go on to produce a black hole, while for smaller values it will eventually disperse into the background medium. For δ close to δ_c (either above or below it) one finds that the compactness $2M/R$ of the collapsing material first decreases, but then attains a value at which it remains for many dynamical timescales. This is the long-lived "intermediate state" and, for a radiation fluid, this has $2M/R \sim 0.5$, quite far from the condition for a black hole. In this state, it sheds matter via a relativistic wind, which is driven by a huge pressure gradient at its surface, and a deep void opens up between it and the rest of the universe. As it loses matter via the wind, it shrinks maintaining an almost constant value of $2M/R$. Eventually, its mass decreases to a point where it begins to deviate from the intermediate state, either collapsing to form a black hole (if $\delta > \delta_c$) or dispersing (if $\delta < \delta_c$). This process was investigated in some detail in Paper 3 for a radiation fluid with $w = 1/3$ and some evidence was seen of self-similar behaviour during the period of the intermediate state. Here, we return to this with the aim of answering two main questions: (i) Does the intermediate state really follow a similarity solution and how does this fit with the surrounding expanding universe? (ii) What is the effect of varying w, and do we find results for this in accordance with earlier calculations, where critical collapse was being studied under simple idealized circumstances rather than following cosmological perturbations within an expanding universe?

When calculations are made, using our approach, for non-standard values of w, there is some artificiality because of having the whole universe following an unusual equation of state and also imposing initial conditions under those circumstances. If one were really considering in detail possible PBH formation with a variant equation of state, one would need a more sophisticated set-up than our present one. However, our aim here is just to get some general indications about the effect of varying w and to make a link with the previous work on critical collapse. We have studied a range of

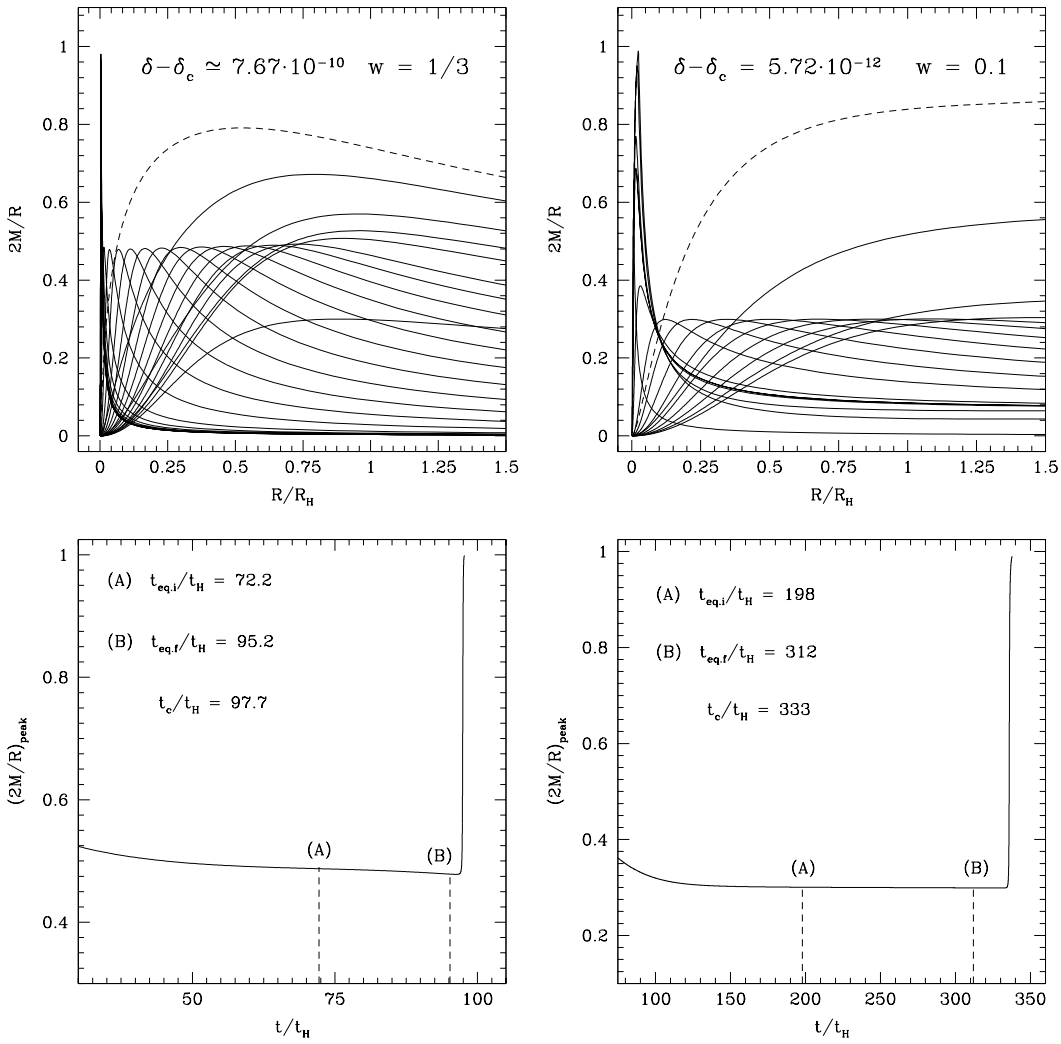

Figure 1. In the top panels the behaviour of $2M/R$ is plotted against R/R_H for a nearly-critical case ($\delta \simeq \delta_c$) for $w = 0.1$ and $w = 1/3$, at different time levels. R_H is the cosmological horizon scale at the moment of horizon crossing. The dashed curve indicates the initial conditions used by the observer-time code. The bottom panels show the time evolution of the peak of $2M/R$ during the intermediate state: t/t_H is the observer time measured in units of the horizon crossing time, while (A) and (B) represent the limits of the time interval used in figure 2, dealing with the self similar solution.

values for w between 0.01 and 0.6, looking at the intermediate state and the scaling law in each case. As w is increased, the features of the relativistic wind and the opening up of the void become progressively more extreme, and this eventually becomes very challenging for the adaptive scheme. It is because of this that we have just used values of $w \leq 0.6$ for the simulations presented here.

We first compare the intermediate state for the standard case of $w = 1/3$ with that for a representative lower value, $w = 0.1$ (and then comment later on what happens for other values). The time spent in the intermediate state becomes progressively longer

as δ approaches δ_c. Figure 1 shows the behaviour of $2M/R$ plotted against R/R_H at different time levels when a black hole is formed with a value of δ extremely close to the threshold (R_H being the cosmological horizon scale at the moment of horizon crossing). The dashed curve shows the initial conditions used by the observer-time code, after which the evolution proceeds in the direction of decreasing $(2M/R)_{peak}$ until the intermediate state is reached, after which the peak moves progressively inwards. When the collapse is extremely close to the critical limit, as it is here, the intermediate state lasts almost up until the formation of the black hole, when $(2M/R)_{peak}$ departs from its almost constant value in the intermediate state and increases up to the black-hole value of 1. Another view of this behaviour is shown in the bottom panels of figure 1, where the time evolution of $(2M/R)_{peak}$ is plotted, for the same two cases as shown in the top panels, starting when the collapse is getting into the intermediate state. One can see that, for the smaller value of w, the intermediate state lasts for longer, with $(2M/R)_{peak}$ being more constant. Note that in both cases the final collapse to form the black hole, when it comes, is extremely rapid in comparison with what has gone before (this is a characteristic feature when δ is close to δ_c). The behaviour for the other values of w which we have tested follows the trends seen for the two cases shown above. We will comment more about this in connection with figure 4 below.

Turning now to the self-similarity, in figure 2 we plot quantities similar to ones used by Evans & Coleman [20] in their study of critical collapse and self-similarity: $2M/R$, $4\pi R^2 e$ and U/c are plotted against $\xi = [R/C(t_c - t)^n]$ at a succession of output times between the points marked with (A) and (B) in figure 2. Here, n is a self-similar exponent, C is a constant ($= R_H/t_c^n$) which makes ξ dimensionless, and t_c is the critical time at which the singularity would be formed in the limiting case $\delta = \delta_c$ (we find t_c in the way described in Paper 3). The time ordering of the curves is from top to bottom on the right hand side for $2M/R$ and $4\pi R^2 e$, and from bottom to top in the mid section for U/c. Evans & Coleman [20] found $n \simeq 1.15$ for the circumstances which they were studying (for a radiation fluid but with a different time-slicing from ours). We calculated best-fit values of n for our calculations and found $n = 0.90$ for $w = 1/3$ and $n = 0.83$ for $w = 0.1$. The self-similarity seen in figure 2 is clearly not exact but represents a rather good approximation for all of the collapsing region out to the peak of $2M/R$ and somewhat beyond. (Note that in the frames for $w = 1/3$, we have purposely included a final time-level where the self-similarity is just starting to break.) Further out, the solutions undergo a transition into the region of the wind and the void where a connection still remains with the surrounding universe. The influence of the connection between the collapsing matter and the surrounding universe is made clear by considering the past light cone of the forming black hole and the eventual singularity (calculated as described in Section 3). The location of the light cone is shown by the vertical dashed lines in figure 2 (there is a slight inward motion of this with respect to ξ during the time shown, indicated by the gap between the two dashed lines). The self-similar region is completely contained within the light cone which, however, also contains material not participating in the self-similarity which can then stop the self-similarity being exact.

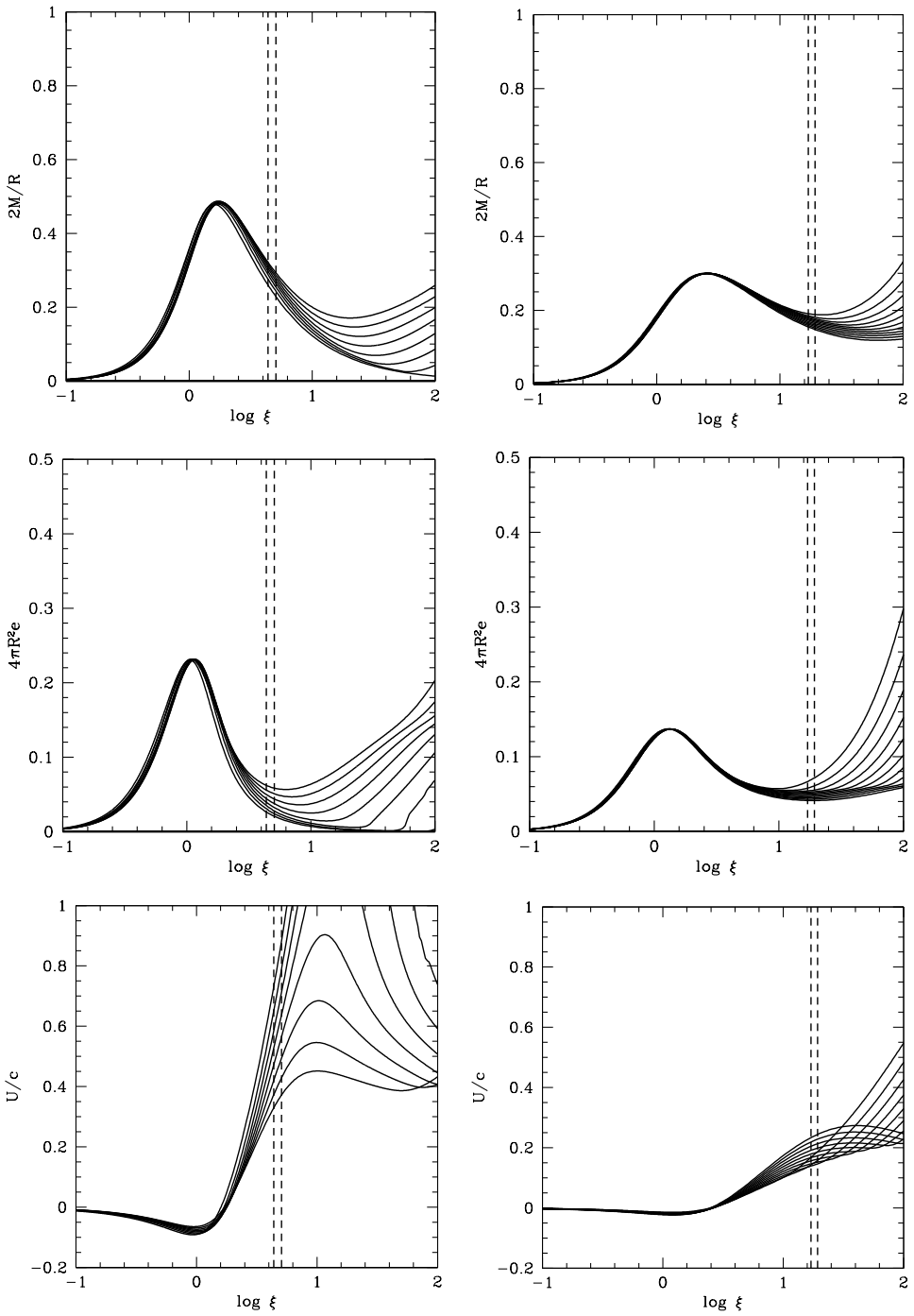

Figure 2. Self-similar behaviour during the intermediate state. For the two cases shown in figure 1, we plot $2M/R$, $4\pi R^2 e$ and U/c against $\xi = [R/C(t_c - t)^n]$ at a succession of output times between the points marked with (A) and (B) in figure 1. The best-fit values for the exponent n are 0.90 for $w = 1/3$ and 0.83 for $w = 0.1$. The vertical dashed lines delimit the small range of variation of the location of the past light-cone (in terms of ξ) during this time; it is slightly moving inward.

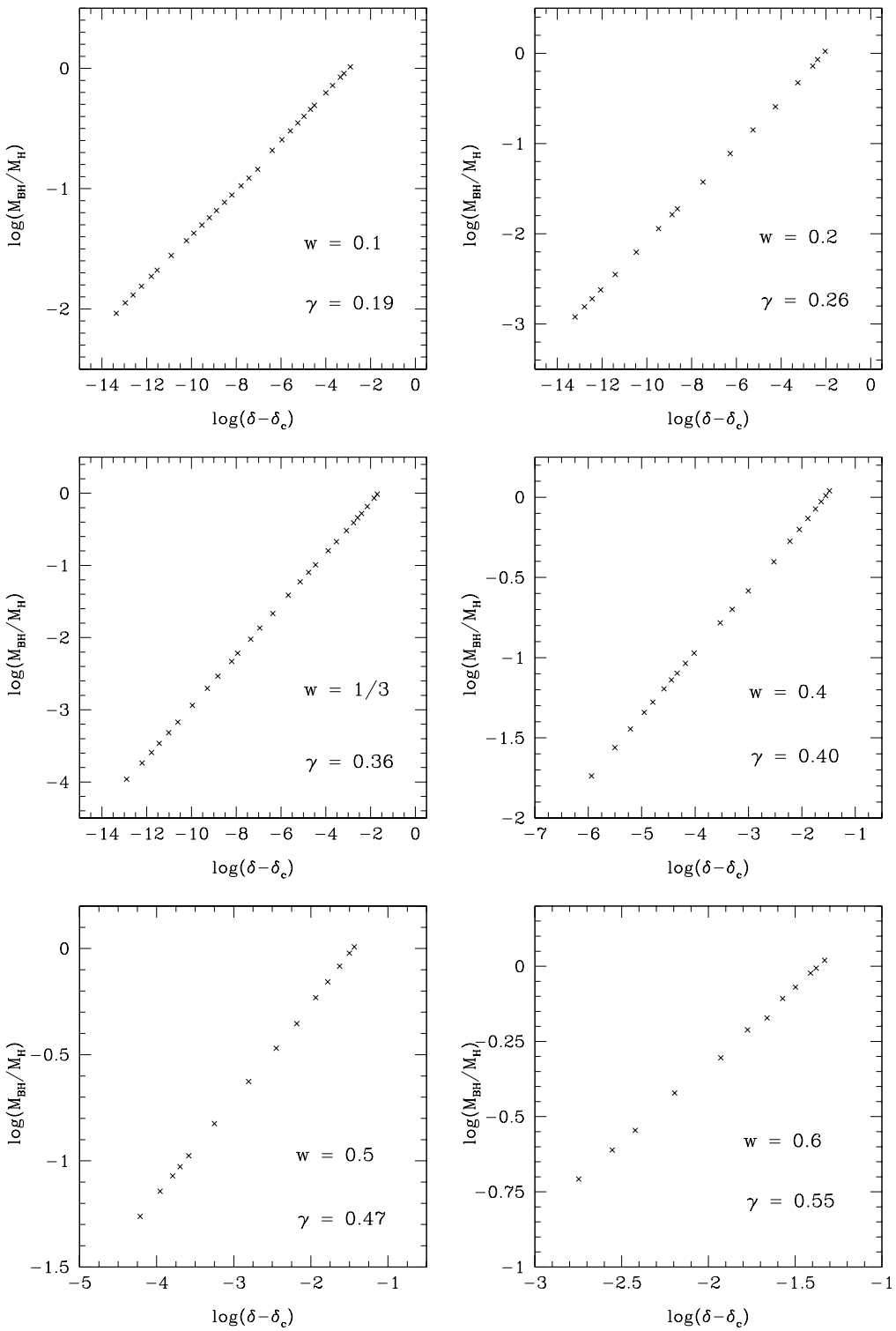

Figure 3. Scaling behaviour for M_{BH} as function of $(\delta - \delta_c)$ for values of w ranging from 0.1 to 0.6; M_H is the cosmological horizon scale at the moment of horizon crossing. The best-fit values for γ are indicated in each case.

The last outputs included in figure 2 are ones just before the deviations away from the approximate self-similarity in the inner regions start to become significant. In the left-hand column, we have actually included one last output where the deviations do start to be clearly seen, as an indication of the behaviour. Note that the breaking of the similarity occurs a little before the final dynamical collapse commences.

In Figure 3 we show the scaling-law behaviour of M_{BH} plotted as a function of $(\delta - \delta_c)$ for several values of w ranging from 0.1 to 0.6. Good scaling laws are obtained in each case over the range of values of $(\delta - \delta_c)$ that we were able to study (note that this range was much smaller in the cases with $w > 1/3$ because of the extreme conditions encountered there). The best-fit values of γ are completely consistent with those obtained previously by Maison [27] and by Neilsen and Choptuik [15] with an imploding shells calculation.

In the left hand panel of figure 4, we show results obtained with our code for the dependence of δ_c on w. Very similar behaviour to this is obtained also for $(2M/R)_{peak}$ during the period of the intermediate state, but with $(2M/R)_{peak}$ being slightly larger than δ_c. The first estimation of the value of δ_c was made in the pioneering paper by Carr [3] in 1975, using an approximate argument based on the Jeans length. He found $\delta_c \sim w$ and our numerical simulations are in reasonable agreement with that, bearing in mind the approximations. This relation between δ_c and w confirms that any epochs in the early universe when the equation of state softens would be favorable for enhancing PBH production. One example of this could be the QCD phase transition, which has previously been discussed in connection with a PBH model for MACHOs [13]. In the right hand panel of figure 4 we plot our values for γ against w, for values of w up to 0.6 (marked with crosses), and this shows a regular behaviour consistent with the limit of

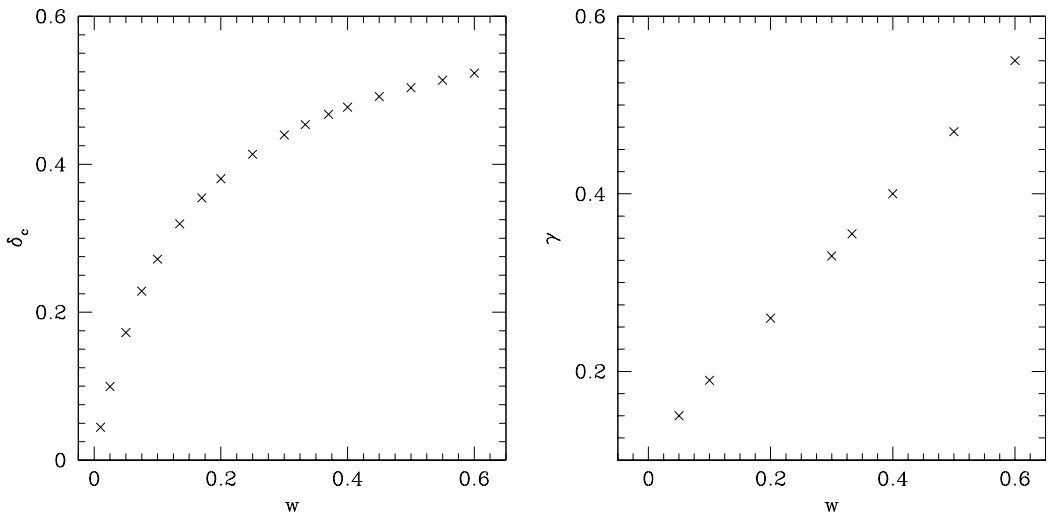

Figure 4. The left-hand plot shows the dependence of δ_c on the value of w, and the right-hand plot shows the behaviour of γ as a function of w (which is almost linear within the range studied here).

$\gamma \to 0.106$ for $w \to 0$ obtained by Snajdr [28]. The values of γ found in our calculations are almost indistinguishable on this scale from those obtained in [27, 15].

Finally we want to comment on one of our earlier results, in Paper 1, where we investigated critical collapse for a radiative fluid also in the presence of a cosmological constant Λ, as described in section 2 here by equations (14) and (15). At the time of Paper 1, the code was not able to get very close to the critical limit because of not yet having the AMR, and the lowest value of $(\delta - \delta_c)$ that we were able to treat was around 10^{-3}. In that regime we found that the presence of a cosmological constant was affecting the scaling law, giving a change in the value of γ in the sense of decreasing it with increasing (positive) Λ. Now, with the present AMR code, we have made similar calculations going down to much smaller values of $(\delta - \delta_c)$ and have seen that this change in γ disappears as one gets closer to δ_c (i.e. the gradients of the two scaling laws converge to the same value). The reason for this is clear: if δ is very close to δ_c, the mass of the black hole is small and the fluid densities involved in forming it are high. Under these circumstances, the energy density related to the cosmological constant becomes negligible in comparison with that of the collapsing fluid. This makes the gradient of the scaling law converge to that without the cosmological constant when $(\delta - \delta_c)$ is sufficiently small. However, the cosmological constant still makes a relevant (and growing) contribution on larger scales where the fluid density is lower.

5. Conclusions

Following on after our previous work investigating primordial black hole formation during the radiative era of the early universe, we have here invested further the critical nature of the collapse in this context, focusing on the long-lived intermediate state, which appears in collapses of perturbations close to the critical limit, and examining the extent to which this follows a similarity solution. This is a key issue, because the presence of a similarity solution is seen as an important characteristic feature of the general phenomenon of critical collapse. Also, we have presented results from calculations where the equation of state parameter w is allowed to take constant values different from the radiative value of 1/3, with the aim gaining further insight into our main case of interest by considering it within a broader context. Our calculations have been made using a purpose-built Lagrangian AMR code, starting with initial supra-horizon scale perturbations of a type which could have come from inflation and then following self-consistently both the collapse to form the black hole and the continuing expansion of the universe.

From our calculations, we have found that a similarity solution does indeed arise in this context, to good approximation, for a region contained within the past light-cone of the forming black hole. The self-similarity is not exact, however, and this is interpreted as being due to the presence within the light-cone of some outer matter still coupled to the expanding universe. We have studied values of w different from 1/3 (up to 0.6) and found that, for cosmological-type perturbations, scaling-law behaviour persists

down to the smallest masses that we are able to follow in each case, with the values obtained for the exponent γ being in almost perfect agreement with those obtained previously by Neilsen and Choptuik [15] from their imploding-shells calculation. The critical threshold amplitude δ_c, the intermediate state compactness $(2M/R)_{peak}$ and the scaling-law exponent γ all vary with w in a way which is easily understandable in view of w being the ratio between the pressure and energy density of the fluid.

Acknowledgments

This work has been partly carried out within the award "Numerical analysis and simulations of geometric wave equations" made under the European Heads of Research Councils and European Science Foundation EURYI (European Young Investigator) Awards scheme, supported by funds from the Participating Organizations of EURYI and the EC Sixth Framework Programme. We gratefully acknowledge helpful discussions, during the course of this work, with a number of colleagues including Bernard Carr, Alexander Polnarev, Carsten Gundlach, Ian Hawke and Karsten Jedamzik, and IM thanks SISSA for giving him use of their facilities.

Appendix: Black-hole and cosmological horizons

In this appendix we discuss how the concepts of black-hole and cosmological horizons emerge from our treatment of light cones. As in the rest of the paper, we assume spherical symmetry and that the medium is a perfect fluid. However, the discussion is general in the sense that it is independent of the equation of state used and we make no assumptions of homogeneity (with reference to the cosmological case), or of asymptotic flatness and the presence of vacuum exteriors (with reference to the black holes). We think that it is interesting to see how well-known results emerge in this approach.

We present the argument with cosmic-time slicing, because it is most transparent when done in this way, but the final conclusions are independent of the slicing and can equally well be demonstrated with the observer time.

First, we consider the conditions for radial null rays (analogous to the discussion in Section 3 for observer time). Recalling that the cosmic-time metric is

$$ds^2 = -a^2\,dt^2 + b^2\,dr^2 + R^2\left(d\theta^2 + \sin^2\theta d\varphi^2\right)\,, \tag{A.1}$$

along radial null rays (for which $ds = d\theta = d\varphi = 0$), we have

$$dr = \pm\frac{a}{b}dt\,, \tag{A.2}$$

where the plus corresponds to an outgoing null ray while the minus is for an ingoing one. The general expression for changes in R along a radial worldline is

$$dR = \frac{\partial R}{\partial t}dt + \frac{\partial R}{\partial r}dr\,, \tag{A.3}$$

and, using the definitions for U and Γ given in expressions (2)-(5), this can be written as

$$dR = aU dt + b\Gamma dr\,. \tag{A.4}$$

Then, inserting condition (A.2) into (A.4), we get the expression for how R changes with time along a radial null ray:

$$\frac{dR}{dt} = a(U \pm \Gamma)\,, \tag{A.5}$$

where the plus is for an outgoing ray while the minus is for an ingoing one. Note that we are working within the co-moving frame of the fluid and so "outgoing" and "incoming" are defined with respect to that frame.

Next, we recall where the constraint equation (13) comes from, giving our expression for Γ. The G^0_0 and G^1_1 components of the Einstein equation give

$$4\pi R^2 e R_{,r} = \frac{1}{2}(R + RU^2 - R\Gamma^2)_{,r}\,, \tag{A.6}$$

and

$$4\pi R^2 apU = -\frac{1}{2}(R + RU^2 - R\Gamma^2)_{,t}\,, \tag{A.7}$$

and one can see the same expression appearing in the parentheses on the right hand side in each case. It is convenient then to make the definition

$$M \equiv \frac{1}{2}(R + RU^2 - R\Gamma^2)\,. \tag{A.8}$$

Integrating equation (A.6) gives

$$M = \int 4\pi R^2 e dR\,, \tag{A.9}$$

(corresponding to the interpretation of M as the mass contained within radius R‡), while (A.7) gives

$$D_t M = -4\pi R^2 pU\,, \tag{A.10}$$

(corresponding to the change of energy resulting from work done against pressure during an adiabatic expansion or contraction). Rearranging the terms in (A.8) then gives the constraint equation (13),

$$\Gamma^2 = 1 + U^2 - \frac{2M}{R}\,. \tag{A.11}$$

Returning now to equation (A.5), the limiting surface at which an outgoing radial light ray (ie outgoing with respect to the matter) cannot move to larger R, is given by

$$\left(\frac{dR}{dt}\right)_{\rm out} = a(U + \Gamma) = 0\,, \tag{A.12}$$

implying

$$\Gamma = -U\,. \tag{A.13}$$

‡ Note that there is an effective cancellation here between Γ factors in both numerator and denominator (see Misner [23]).

This corresponds to the apparent horizon of a black hole. Similarly, the limiting surface at which an incoming radial light ray (with respect to the matter) cannot move to smaller R is given by

$$\left(\frac{dR}{dt}\right)_{\rm in} = a(U-\Gamma) = 0\,, \tag{A.14}$$

implying

$$\Gamma = U\,. \tag{A.15}$$

This corresponds to the cosmological horizon. Conditions (A.13) and (A.15) are different, of course, but both correspond to

$$\Gamma^2 = U^2\,, \tag{A.16}$$

and then, using (A.11), to

$$R = 2M\,. \tag{A.17}$$

As noted above, this familiar result (equivalent to that in the Schwarzschild solution) is independent of the slicing used and does not require assumptions of homogeneity (with reference to the cosmological case), or of asymptotic flatness and the presence of vacuum exteriors (with reference to black holes).

References

[1] Zel'dovich Ya.B. & Novikov I.D. 1966 *Astron.Zh.* **43** 758 [*Sov.Astron.* **10** 602 (1967)]
[2] Hawking S.W. 1971 *MNRAS* **152** 75
[3] Carr B.J. & Hawking S.W. 1974 *MNRAS* **168**, 399
[4] Carr B.J. 1975 *Astrophys.J.* **201** 1
[5] Nadezhin D.K., Novikov I.D. & Polnarev A.G. 1978 *Sov.Astron.* **22(2)** 129
[6] Bicknell G.V. & Henriksen R.N. 1979 *Astrophys.J.* **232** 670
[7] Novikov I.D. & Polnarev A.G. 1980 *Sov.Astron.* **24(2)** 147
[8] Niemeyer J.C. & Jedamzik K. 1999 *Phys.Rev.D* **59** 124013
[9] Shibata M. & Sasaki M. 1999 *Phys.Rev.D* **60** 084002
[10] Hawke I. & Stewart J.M. 2002 *Class. Quantum Grav.* **19** 3687
[11] Musco I., Miller J.C., Rezzolla L. 2005 *Class. Quantum Grav.*, **22**, 1405
[12] Niemeyer J.C. & Jedamzik K. 1998 *Phys.Rev.Lett* **80** 5481
[13] Jedamzik K. & Niemeyer J.C. 1999 *Phys.Rev.D* **59** 124014
[14] Choptuik M.W. 1993 *Phys. Rev. Lett.* **70** 9
[15] Neilsen D.W. & Choptuik M.W. 2000 *Class. Quantum Grav.*, **17**, 761
[16] Polnarev A.G. & Musco I. 2007 *Class. Quantum Grav.*, **24**, 1405
[17] Lifshitz E.M. & Khalatnikov I.M. 1963 *Usp. Fiz. Nauk.* **80**, 391 [*Sov. Phys. Usp.* **6**, 495 (1964)]
[18] Lyth D.H., Malik K.A., Sasaki M. 2005 *JCAP* **May** 004
[19] Musco I., Miller J.C., Polnarev A.G. 2009 *Class. Quantum Grav.*, **26**, 235001
[20] Evans C.R. & Coleman J.S. 1994 *Phys. Rev. Lett.* **72** 1782
[21] Gundlach C. & Martín-García J.M. 2007 *Living Rev. Relativity* **5** [`http://www.livingreviews.org/lrr-2007-5`]
[22] Misner C.W. & Sharp D.H. 1964 *Phys.Rev* **136** B571
[23] Misner C.W. 1969, in "Astrophysics and General Relativity, Volume 1, 1968 Brandeis University Summer Institute in Theoretical Physics" Eds. M. Chrêtien, S. Deser and J. Goldstein (Gordon and Breach, New York), p.113

[24] Hernandez W.C. & Misner C.W. 1966 *Astrophys.J.* **143** 452
[25] Miller J.C. & Motta S. 1989 *Class. Quantum Grav.* **6** 185
[26] Miller J.C. & Rezzolla L. 1995 *Phys.Rev.D* **51** 4017
[27] Maison D. 1996 *Phys. Lett. B* **366** 82
[28] Snajdr M. 2006 *Class. Quantum Grav.* **23** 3333